

# The effect of longitudinal spin-fluctuations on high temperature properties of $\text{Co}_3\text{Mn}_2\text{Ge}$

Erna K. Delczeg-Czirjak,<sup>1,\*</sup> O. Eriksson,<sup>1,2</sup> and A. V. Ruban<sup>3,4</sup>

<sup>1</sup>*Department of Physics and Astronomy, Uppsala University, Box 516, SE-75120 Uppsala, Sweden*

<sup>2</sup>*School of Science and Technology, Örebro University, SE-70182 Örebro, Sweden*

<sup>3</sup>*Department of Materials Science and Engineering,*

*KTH Royal Institute of Technology, SE-100 44 Stockholm, Sweden*

<sup>4</sup>*Materials Center Leoben Forschung GmbH, A-8700 Leoben, Austria*

(Dated: June 1, 2022)

It is demonstrated that thermally induced longitudinal spin fluctuations (LSF) play an important role in itinerant  $\text{Co}_3\text{Mn}_2\text{Ge}$  at an elevated temperature. The effect of LSF is taken into account during *ab initio* calculations via a simple model for the corresponding entropy contribution. We show that the magnetic entropy leads to the appearance of a medium size local moment on Co atoms. As a consequence, this leads to a renormalization of the magnetic exchange interactions with a quite substantial impact upon the calculated Curie temperature. Taking LSF into account, the calculated Curie temperature can be brought to be in good agreement with the experimental value.

## I. INTRODUCTION

Recent studies show that high-throughput density functional theory (DFT) approach [1–7] can be effective in filtering through a large number of compounds in the search for new high-performance RE free permanent magnets or magnetocaloric materials, which would be time-consuming and expensive to synthesize experimentally. Curie temperature is one of the very important parameters for permanent magnets and magnetocaloric materials filtering, which can be determined or at least qualitatively estimated in *ab initio* calculations.

Within a DFT consideration, the Curie temperature is routinely obtained using an additional statistical consideration based either on the energy difference of magnetic structures or via magnetic exchange interactions of a magnetic Hamiltonian. Although classical Heisenberg Hamiltonian suffices to perform relatively accurate calculations of the Curie temperature, the main problem in this approach may arise from the strong sensitivity of the magnetic exchange interactions, for instance, as they are defined within the magnetic force theorem [8], to the magnetic state [9], which is also reflected in some cases in the strong dependence of the local magnetic moment on the magnetic configuration [10].

This basically means that such a Hamiltonian cannot be used for such a system within the whole range of temperatures and global magnetic states, at least if one requires that its parameters should not depend on a particular magnetic configuration, something which is the topic of recent discussions [9, 11, 12]. Nevertheless, the whole formalism of a classical Heisenberg Hamiltonian can still make sense and produce reasonably accurate results when it is applied within a limited range of external parameters (temperature and pressure) and for a restricted set

of magnetic configurations. In this case, magnetic exchange interactions should be determined at the corresponding conditions and in the corresponding magnetic state. In particular, since magnetic phase transitions are commonly of the second order, one could argue that the corresponding magnetic exchange interactions should be determined in the paramagnetic state, to which such a transition happens.

This is in fact the reason why the calculated Curie temperature of  $\text{Co}_3\text{Mn}_2\text{Ge}$  [1] using magnetic exchange interactions obtained from the ordered, ferromagnetic state, 750 K, was found to be twice as high as the experimental one [1], 359 K. Considering the fact that the account of the experimentally observed chemical disorder between Co and Ge did not improve the theoretical results, we assume here that the main source of the discrepancy in [1] is the strong dependence of magnetic interactions on the magnetic state. In other words, they are substantially different from the interactions in paramagnetic state next to the point of magnetic phase transition.

The main reason for the quite strong dependency of the magnetic interactions in  $\text{Co}_3\text{Mn}_2\text{Ge}$  on the temperature and magnetic state is its itinerant magnetism, especially related to Co atoms. In the usual disordered local moment (DLM) *ab initio* zero K calculations [13, 14] modeling paramagnetic state, the magnetic moment of Co atoms becomes too small, while at finite temperature, its magnitude is strongly affected by the LSF, which can be considered as thermal excitation due to specific entropy related to this degree of freedom [15–20]. The strong itinerant nature of Co moments and the localization of Mn moments indicate a potential of  $\text{Co}_3\text{Mn}_2\text{Ge}$  as magnetocaloric material similarly to  $\text{Fe}_2\text{P}$  based alloys [21, 22].

In this paper, we account for LSF in the paramagnetic state and calculate the Curie temperature of  $\text{Co}_3\text{Mn}_2\text{Ge}$  using the corresponding magnetic exchange interactions. The theoretical model and details of calculations are described in the next section.

---

\* erna.delczeg@physics.uu.se

## II. THEORETICAL TOOLS

### A. Magnetic model

A Heisenberg classical magnetic Hamiltonian is used for the corresponding statistical thermodynamics simulations done using Monte Carlo (MC) method. In a general form, see for instance [19], it allows for fluctuation of the magnitude of magnetic moments on each site of the lattice, and thus it contains on-site terms as well as pair interaction contribution, which depends on specific local magnetic moments at the corresponding sites and the average local magnetic moment of the whole system.

In the case of alloys, such an approach becomes quite cumbersome. Nevertheless, it can be significantly simplified without loosing much of the accuracy using its mean-field-like consideration for the task of finding the Curie temperature, which can be done for the restricted range of temperatures.

First of all, one can neglect the general temperature dependence of the magnetic exchange interactions, connected with the temperature dependence of the LSF, by considering one particular temperature, which is close to the experimentally known or "theoretically expected" Curie temperature. Secondly, although the fluctuation of local magnetic moments can be quite large, some tests done for several pure metals (Ni, Co, and Fe) show that the use of *average* local magnetic moments (for some temperature and other external parameters) produces quite close results to the "fluctuating" consideration. These allow one to simplify magnetic Hamiltonian to its usual form for alloys [23]:

$$H = - \sum_p \sum_{i,j \in p} \sum_{\alpha, \beta = \text{Co1, Co2, Mn}} J_p^{\alpha\beta} c_i^\alpha c_j^\beta \mathbf{e}_i \mathbf{e}_j. \quad (1)$$

Here,  $J_p^{\alpha\beta}$  are the magnetic exchange interactions between  $\alpha$  and  $\beta$  alloy components for coordination shell  $p$  and  $\mathbf{e}_i$  is the direction of the spin at site  $i$ ;  $c_i^\alpha$  takes on value 1 if site  $i$  is occupied by atom  $\alpha$  and 0 otherwise.

Statistical thermodynamics simulations of the magnetic phase transition were done by MC method implemented within the Uppsala atomistic spin dynamics (UpASD) software [24, 25]. MC simulations were performed on a  $40 \times 40 \times 40$  supercell with periodic boundary conditions. The size and direction of the magnetic moments were chosen randomly at each MC trial and 10000 MC steps were used for equilibration followed then by 50000 steps for obtaining thermodynamic averages.

### B. Electronic structure and magnetic exchange interactions

Electronic structure calculations were done by the exact muffin-tin orbital (EMTO) method [26, 27] where the

chemical and magnetic disorder is treated within the coherent potential approximation (CPA) [28, 29] (EMTO-CPA [30]). The electrostatic correction to the single-site CPA was considered as implemented in the Lyngby version of the EMTO code [31]. For details the reader is referred to Refs. [31], [32], and [33].

The one-electron Kohn-Sham equations were solved within the soft-core and scalar-relativistic approximations, with  $l_{\max} = 3$  for partial waves and  $l_{\max}^t = 5$  for their "tails". The Green's function was calculated for 16 complex energy points distributed exponentially on a semi-circular contour including states within 1.1 Ry below the Fermi level. The exchange-correlation effects was described within the local spin-density approximation [34, 35]. Magnetic exchange interactions were calculated within the magnetic force theorem [8] as implemented in the Lyngby version of the EMTO-CPA code [31].

For "magnetic" alloy components, i.e. Co and Mn, the DLM configuration was used in calculations within CPA. To account for the LSF, we used the following approximation for the magnetic entropy [36]:

$$S_{\text{mag}} = d \ln(m), \quad (2)$$

where  $m$  is local magnetic moment of an atom in the paramagnetic state,  $d = 1, 2, \text{ or } 3$ , (case 1, 2, or 3 considered below) for the component in high-, medium-, or low-spin states leading to different coupling between longitudinal and transverse fluctuations of magnetic moment at finite temperatures (at least above the magnetic transition).

These expressions can be derived assuming a quadratic form for the LSF energy with respect to the magnitude of the local magnetic moment following the recipe of Ref. [20]. The LSF energy can be determined in the DLM calculations. Case 3 corresponds to the full coupling between longitudinal and transverse fluctuations, i.e. when local magnetic moment at finite temperature in the paramagnetic state can exist only due to LSF. In this case, the minimum of the LSF energy is at  $m = 0$ , like for pure Ni, [19]. Case 1 corresponds to a weak coupling, when longitudinal and transverse fluctuations are little independent, and case 2 is an intermediate case.

All calculations were performed for the experimental structure and composition given in Ref. [1].  $\text{Co}_3\text{Mn}_2\text{Ge}$  crystallizes in a hexagonal structure with space group P63/mmc (number 194) with  $a = 4.8032$  and  $c = 7.7378$  lattice parameters, respectively. The actual composition is  $\text{Co}_{3.39}\text{Mn}_2\text{Ge}_{0.61}$  with a considerable intermixing between Co and Ge, as follows: 84 at. % Co (labeled as Co1 on Fig.1 and thereafter) and 16 at. % of Ge occupy the  $6h$  position, 74 at. % of Co (labeled as Co2 on Fig.1 and thereafter) and 26 at. % Ge occupy the  $2a$  position, and Mn exclusively occupies the  $4f$  position. Magnetic measurements show a non-collinear magnetic structure for  $\text{Co}_{3.39}\text{Mn}_2\text{Ge}_{0.61}$  below 200 K and the ferromagnetic one above that up to the Curie temperature at 359 K.

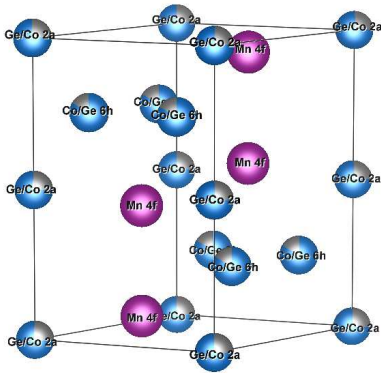


FIG. 1: (Color online) Experimental structure of  $\text{Co}_3\text{Mn}_2\text{Ge}$  from Ref. [1] generated by VESTA code [37].

### III. RESULTS

To identify the type of magnetic behaviour of Co and Mn in paramagnetic calculations, we calculate the LSF energy,  $E_{\text{LSF}}(m_i)$ , in the paramagnetic (DLM) state fixing the magnitude of the magnetic moment of the corresponding alloy component while the others are relaxed to their "equilibrium" magnitudes. It is shown in Fig. 2 for Co1, Co2, and Mn. Clearly, its behaviour differs substantially for Co and Mn: in the case of Mn, it has a deep and pronounced minimum at  $m_{\text{Mn}} = 3.05 \mu_B$ , which is very close to its magnitude in the FM ground state,  $3.26 \mu_B$ , while the latter is quite shallow for both Co atoms. Obviously, Mn in this system is in a more localized magnetic state, and it is not susceptible to LSF at finite temperatures. This behaviour is in fact rather similar to that of the  $\text{Fe}_2\text{P}$  based magneto caloric materials [21, 22]. Ref. [21] shows that Fe moment on the tetrahedral  $3f$  site of  $\text{Fe}_2\text{P}$  is quite sensitive to the magnetic environment, while the Fe moment on the octahedral  $3g$  site is robust. This fact leads to a strong temperature dependence of the magnetic moments and at last is responsible for the first order nature of the magnetic transition and finally manifest in a large magnetocaloric effect in  $\text{Fe}_2\text{P}$  and related compounds [22].

At the same time, the  $T=0$  K local moments of Co1 and Co2 are  $0.44$  and  $0.12 \mu_B$ , respectively, while their magnitudes in the FM ground state are substantially higher:  $1.60$  and  $1.57 \mu_B$ . These means that LSF should affect the magnetic moment of Co quite strongly, especially taking into consideration the flat character of  $E_{\text{LSF}}(m_i)$  around the minimum.

To illustrate the effect of LSF at finite temperature on the magnitudes of local magnetic moments of Co and Mn, we perform DLM-LSF calculations at the experimental transition temperature  $359$  K using 3 different cases determined in the previous section. The results are listed in Table I. As one can see, the magnetic moments

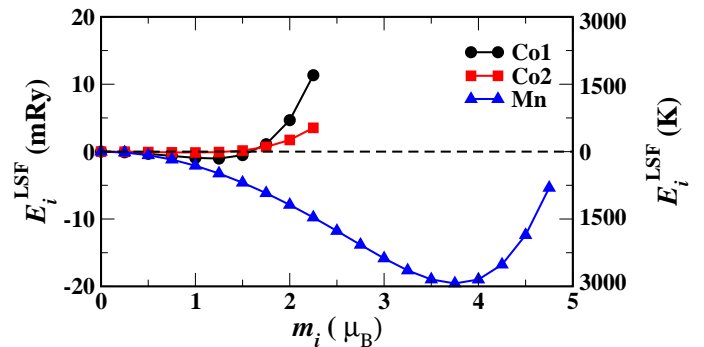


FIG. 2: (Color online) Longitudinal spin fluctuation energy ( $E_i^{\text{LSF}}$ ) as a function of the local moment ( $m_i$ ) of Co1 (black circles), Co2 (red squares), and Mn (blue triangles), respectively obtained in zero K DLM calculations. The energy scale is given in mRy units (left) and absolute temperature (right).

of Co change drastically with including LSF at even quite moderate temperature in all three cases, although they are still lower in magnitude compared to their values of the FM state. At the same time, the magnetic moment of Mn in the DLM-LSF calculations at  $359$  K is practically the same as in DLM  $T=0$  K calculations.

TABLE I: Element and site resolved magnetic moments ( $m_i$  in  $\mu_B$ ) and theoretically estimated Curie temperatures ( $T_C$  in K) for  $\text{Co}_{3.39}\text{Mn}_2\text{Ge}_{0.61}$  in different magnetic states: FM, DLM, and LSF-DLM for case 1, 2, and 3.

$m_i$	FM	DLM	LSF-1	LSF-2	LSF-3
Co1	1.60	0.44	0.89	1.03	1.12
Co2	1.57	0.12	0.86	1.02	1.11
Mn	3.26	3.05	3.01	2.99	2.97

The effect of LSF on the local magnetic moments at finite temperature translates to the values of the corresponding magnetic exchange interactions. In Fig. 3, we present magnetic exchange interactions obtained in different magnetic states: FM (black circles), DLM (red squares), and DLM-LSF1 (labelled LSF, green triangles) at  $359$  K, as a function of interatomic distance. As one can see, the strongest interactions in the FM state are for between Co1-Co1 and Co1-Co2 atoms at the first two coordination shells and they are of ferromagnetic type. The  $\text{Co}_i$ -Mn interaction at the first coordination shell is just a bit smaller than those interactions and it is also of the ferromagnetic type. The Co2-Co2 magnetic exchange interactions are very small and they can hardly influence the magnetic configuration at finite temperature. The Mn-Mn interactions are also small and negative, i.e. it is of antiferromagnetic type. Obviously, such interactions should strongly stabilize the FM state at  $0$  K, which is not the ground state for this particular alloy configuration.

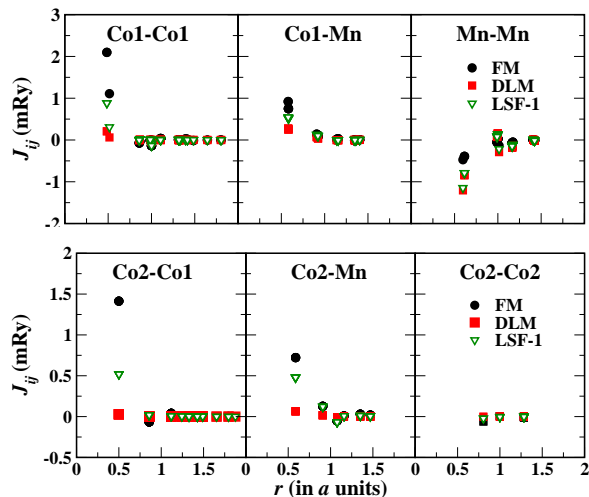


FIG. 3: (Color online) Magnetic exchange interactions between the magnetic elements calculated for the three reference states. Black filled circles stand for FM, red filled squares denote DLM and open green triangles stand for case 1 LSF at 359 K, respectively.

The situation is quite different in the DLM state without LSF. All Co-Co and Co-Mn interactions become insignificant, while the negative  $J^{\text{MnMn}}$  at the first several coordination shells strengthens. Clearly, this type of interactions cannot provide the stabilization of the FM state, and one can expect a stabilization either of a certain type of antiferromagnetic or non-collinear state. The DLM-LSF-1 magnetic exchange interactions at 359 K have somewhat intermediate values for  $\text{Co}_i\text{-Co}_i$  and  $\text{Co}_i\text{-Mn}$ , compared to those in the FM and DLM states. At the same time,  $J^{\text{Mn-Mn}}$  are practically the same as in the DLM state, which is quite expected.

The magnetic exchange interactions obtained for different magnetic states (also including LSF-2, and LSF-3 cases) were used in Monte Carlo simulations of the magnetic phase transition. In Fig. 4, we show the normalized magnetic susceptibility from these simulations,  $\chi_{\text{norm}}$ , for  $\text{Co}_{0.39}\text{Mn}_{0.61}\text{Ge}$  obtained different sets of  $(J_p^{\alpha,\beta})$ . The susceptibility peaks correspond to the magnetic transition at the corresponding temperature,  $T_C$ , which are also listed in Table II. As is clear from Fig. 4, the FM magnetic exchange interactions considerably overestimate  $T_C$  compared to the experimental data (359 K) [1].

TABLE II: Calculated Curie temperature for magnetic interactions determined in different magnetic states.

State	FM	DLM	LSF-1	LSF-2	LSF-3
$T_C$	750	-	345	460	545

At the same time, DLM-LSF interactions produce quite good results, especially in the DLM-LSF-1 case (DLM results are not shown since they produce wrong ground state and very low transition temperature). Al-

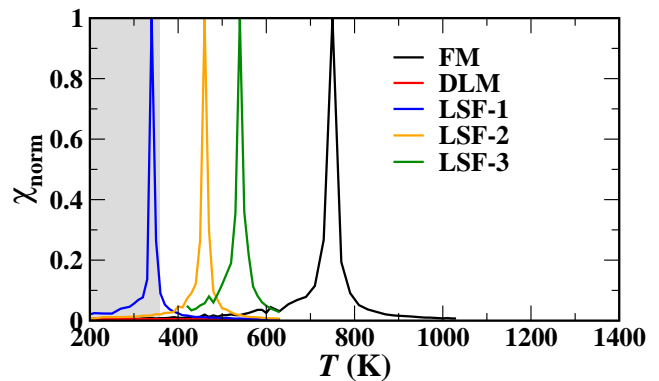


FIG. 4: (Color online) Normalised magnetic susceptibility calculated for different reference states. Grey shaded area indicates the experimental ferromagnetic state.

though LSF-2 interactions produce higher Curie temperature than experimental data, these results are still reasonable taking into consideration that fact that the present simulations involve several practically unavoidable assumptions and approximations.

First of all, the model of LSF is quite rough: it is based on an heuristic classical picture of magnetism within one-electron DFT at  $T=0$  K. Moreover, we do classical Heisenberg Monte Carlo simulations, where the LSF degree of freedom is "hard-coded" in the corresponding effective interactions. There are some approximations concerning the structure of the system too. Although we use experimental information about distribution of atoms between sublattices, the latter is not completely certain since it is based on a fitting procedure involving some specific assumptions. We use random distribution of Co and Ge atoms on their sublattices, which just comes out from a random number generator in our MC simulations. At the same time, Co and Ge atoms in real alloys most probably have some specific atomic short range order. Finally, our magnetic exchange interactions are determined at the ideal, i.e. unrelaxed, lattice positions neglecting possible local atomic relaxations related to the size mismatch of Co and Ge.

#### IV. CONCLUSIONS

We have calculated the Curie temperature for disordered  $\text{Co}_3\text{Mn}_2\text{Ge}$  in Monte Carlo simulations using magnetic exchange interactions for pairs of Co and Mn atoms obtained in first principles calculations for different magnetic states: FM, DLM, and DLM-LSF with different degrees of coupling at 359 K. The FM interactions considerably overestimate the transition temperature, while the DLM interactions are too weak to produce reasonable results for magnetic transition. The large difference between FM and DLM values of  $T_C$  is due to the non-Heisenberg behavior of the system, i.e. the large differ-

ence between the FM and the DLM local moments of the Co atoms.

The failure of these two schemes is cured by account of thermally induced longitudinal spin-fluctuations for Co atoms, which exhibit weak itinerant magnetism in this system. The effect of LSF is taken into account during the *ab initio* calculations via a simple model that includes the effect of thermally induced magnetic entropy on local moments and consequently on  $J^{\alpha\beta}$ s. We show that the LSF contribution is crucial for reconciliation of the theory and experimental data for the Curie temperature. This scheme is computationally very efficient and easy to include to a high-throughput approach in searching new candidates of permanent-magnet or magnetocaloric materials.

On the other hand, the strong dependence of the Co moments on the magnetic configuration, as a consequence on the temperature, and the stability of Mn moments, indicate a promising magneto caloric potential of this material at room temperature similarly to Fe<sub>2</sub>P based materials [21, 22].

#### ACKNOWLEDGEMENTS

The authors thank the Swedish Foundation for Strategic Research (SSF), project "Magnetic materials for green

energy technology" (contract EM-16-0039) for financing this project. STandUPP and eSSENCE are acknowledged for financial support and the Swedish National Infrastructure for Computing (SNIC) for computational resources (snic2021-1-36 and snic2021-5-340). O.E. also acknowledges support from the Swedish Research Council (VR) and the Knut and Alice Wallenberg foundation (KAW). Some DFT simulations were performed on resources provided by the Swedish National Infrastructure for Computing (SNIC) at PDC (Stockholm) and NSC (Linköping). AVR acknowledges a European Research Council grant, the VINNEX center Hero-m, financed by the Swedish Governmental Agency for Innovation Systems (VINNOVA), Swedish industry, and the Royal Institute of Technology (KTH). AVR also gratefully acknowledges the financial support under the scope of the COMET program within the K2 Center "Integrated Computational Material, Process and Product Engineering (IC-MPPE)" (Project No 859480). This program is supported by the Austrian Federal Ministries for 718 Climate Action, Environment, Energy, Mobility, Innovation and Technology (BMK) and for Digital and Economic Affairs (BMDW), represented by the Austrian research funding association (FFG), and the federal states of Styria, Upper Austria and Tyrol.

- 
- [1] A. Vishina, D. Hedlund, V. Shtender, E. K. Delczeg-Czirjak, S. R. Larsen, O. Y. Vekilova, S. Huang, L. Vitos, P. Svedlindh, M. Sahlberg, O. Eriksson, and H. C. Herper, *Acta Materialia* **212**, 116913 (2021).
- [2] A. Vishina, O. Y. Vekilova, T. Björkman, A. Bergman, H. C. Herper, and O. Eriksson, *Phys. Rev. B* **101**, 094407 (2020).
- [3] I. Batashev, G. A. de Wijs, and E. Brück (Elsevier, 2021) pp. 1–39.
- [4] J. D. Bocarsly, E. E. Levin, C. A. C. Garcia, K. Schwennicke, S. D. Wilson, and R. Seshadri, *Chemistry of Materials* **29**, 1613 (2017), <https://doi.org/10.1021/acs.chemmater.6b04729>.
- [5] J. D. Bocarsly, E. E. Levin, C. A. C. Garcia, K. Schwennicke, S. D. Wilson, and R. Seshadri, *Chemistry of Materials* **29**, 1613 (2017), <https://doi.org/10.1021/acs.chemmater.6b04729>.
- [6] C. E. Calderon, J. J. Plata, C. Toher, C. Oses, O. Levy, M. Fornari, A. Natan, M. J. Mehl, G. Hart, M. Buongiorno Nardelli, and S. Curtarolo, *Computational Materials Science* **108**, 233 (2015).
- [7] C. A. C. Garcia, J. D. Bocarsly, and R. Seshadri, *Phys. Rev. Materials* **4**, 024402 (2020).
- [8] A. I. Liechtenstein, M. I. Katsnelson, and V. A. Gubanov, *Journal of Physics F: Metal Physics* **14**, L125 (1984).
- [9] A. V. Ruban, S. Shallcross, S. I. Simak, and H. L. Skriver, *Phys. Rev. B* **70**, 125115 (2004).
- [10] S. Shallcross, A. E. Kissavos, V. Meded, and A. V. Ruban, *Phys. Rev. B* **72**, 104437 (2005).
- [11] R. Cardias, A. Szilva, A. Bergman, Y. Kvashnin, J. Fransson, S. Streib, A. Delin, M. I. Katsnelson, D. Thonig, A. B. Klautau, O. Eriksson, and L. Nordström, *Phys. Rev. B* **105**, 026401 (2022).
- [12] M. dos Santos Dias, S. Brinker, A. Lászlóffy, B. Nyári, S. Blügel, L. Szunyogh, and S. Lounis, *Phys. Rev. B* **103**, L140408 (2021).
- [13] A. J. Pindor, J. Staunton, G. M. Stocks, and H. Winter, *Journal of Physics F: Metal Physics* **13**, 979 (1983).
- [14] B. L. Gyorffy, A. J. Pindor, J. Staunton, G. M. Stocks, and H. Winter, *Journal of Physics F: Metal Physics* **15**, 1337 (1985).
- [15] J. B. Staunton and B. L. Gyorffy, *Phys. Rev. Lett.* **69**, 371 (1992).
- [16] M. Uhl and J. Kübler, *Phys. Rev. Lett.* **77**, 334 (1996).
- [17] N. M. Rosengaard and B. Johansson, *Phys. Rev. B* **55**, 14975 (1997).
- [18] J. Kübler, *Theory of Itinerant Electron Magnetism* (Clarendon, Oxford, 2000).
- [19] A. V. Ruban, S. Khmelevskiy, P. Mohn, and B. Johansson, *Phys. Rev. B* **75**, 054402 (2007).
- [20] A. V. Ruban, A. B. Belonoshko, and N. V. Skorodumova, *Phys. Rev. B* **87**, 014405 (2013).
- [21] E. K. Delczeg-Czirjak, L. Bergqvist, O. Eriksson, Z. Gercsi, P. Nordblad, L. Szunyogh, B. Johansson, and L. Vitos, *Phys. Rev. B* **86**, 045126 (2012).
- [22] N. H. Dung, Z. Q. Ou, L. Caron, L. Zhang, D. T. C. Thanh, G. A. de Wijs, R. A. de Groot, K. H. J. Buschow, and E. Brück, *Advanced Energy Materials* **1**, 1215 (2011),

- <https://onlinelibrary.wiley.com/doi/pdf/10.1002/aenm.201102110>
- [23] A. V. Ruban, Phys. Rev. B **95**, 174432 (2017).
- [24] B. Skubic, J. Hellsvik, L. Nordstrom, and O. Eriksson, J. Phys.: Condens. Matter **20**, 315203 (2008).
- [25] O. Eriksson, A. Bergman, L. Bergqvist, and J. Hellsvik, *Atomistic Spin Dynamics, Foundations and Applications* (Oxford University Press, 2016).
- [26] O. K. Andersen, O. Jepsen, and G. Krier, *Lectures on Methods of Electronic Structure Calculation, Engineering Materials and Processes* (World Scientific, Singapore, 1994).
- [27] L. Vitos, *The EMTO Method and Applications, in Computational Quantum Mechanics for Materials Engineers, Engineering Materials and Processes* (Springer-Verlag London, 2007).
- [28] P. Soven, Phys. Rev. **156**, 809 (1967).
- [29] B. L. Gyorffy, Phys. Rev. B **5**, 2382 (1972).
- [30] L. Vitos, I. A. Abrikosov, and B. Johansson, Phys. Rev. Lett. **87**, 156401 (2001).
- [31] A. V. Ruban and M. Dehghani, Phys. Rev. B **94**, 104111 (2016).
- [32] A. V. Ruban and H. L. Skriver, Phys. Rev. B **66**, 024201 (2002).
- [33] A. V. Ruban, S. I. Simak, P. A. Korzhavyi, and H. L. Skriver, Phys. Rev. B **66**, 024202 (2002).
- [34] J. P. Perdew and Y. Wang, Phys. Rev. B **45**, 13244 (1992).
- [35] D. M. Ceperley and B. J. Alder, Phys. Rev. Lett. **45**, 566 (1980).
- [36] A. Ruban, Computational Materials Science **187**, 110080 (2021).
- [37] K. Momma and F. Izumi, Journal of Applied Crystallography **44**, 1272 (2011).